

Site-Directed Mutagenesis Studies on the Toluene Dioxygenase Enzymatic System: Role of Phenylalanine 366, Threonine 365 and Isoleucine 324 in the Chemo-, Regio-, and Stereoselectivity

María Agustina Vila,^a Diego Umpiérrez,^a Nicolás Veiga,^b Gustavo Seoane,^a Ignacio Carrera,^{a,*} and Sonia Rodríguez Giordano^{a,*}

^a Laboratorio de Biotálisis y Biotransformaciones, Departamento de Química Orgánica–Departamento de Biociencias, Facultad de Química, Universidad de la República, Montevideo, Uruguay
Tel: + 59829244543

Fax: + 59829241906; e-mail: icarrera@fq.edu.uy; soniar@fq.edu.uy

^b Química Inorgánica, Departamento Estrella Campos, Facultad de Química, Universidad de la República, Montevideo, Uruguay

Received: April 7, 2017; Revised: April 29, 2017; Published online: May 29, 2017

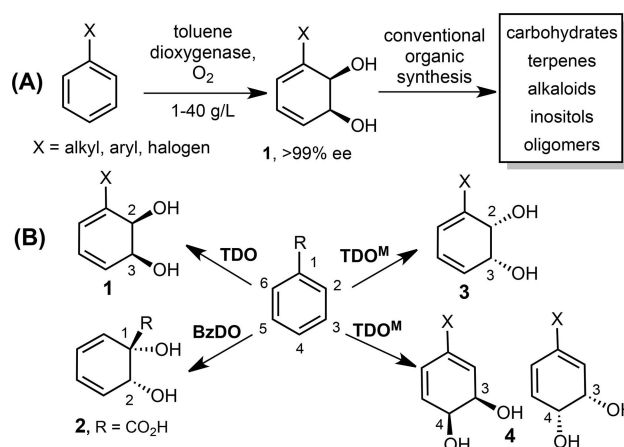


Supporting information for this article is available on the WWW under <https://doi.org/10.1002/adsc.201700444>

Abstract: Toluene Dioxygenase (TDO) enzymatic complex has been widely used as a biocatalyst for the regio- and enantioselective preparation of *cis*-cyclohexadienediols, which are very important starting materials for organic synthesis. However, the lack of regio- and stereodiversity of the dioxygenation process by TDO and related dioxygenases constitutes a clear drawback when planning the use of these diols in synthetic schemes. In this work, we developed three TDO mutants in residues phenylalanine 366, threonine 365 and isoleucine 324, with the aim to alter the chemo-, regio- and stereoselectivity of the biotransformation of arenes. While no changes in the regioselectivity of the process were observed, dramatic variations in the chemo- and enantioselectivity were found for mutants I324F, T365N and F366 V in a substrate-dependent manner.

Keywords: Toluene dioxygenase; *cis*-cyclohexadienediols; Rieske dioxygenases; site-directed mutagenesis

and efficient synthetic schemes. This has been highlighted in several reviews, which show the importance of these dienediols for enantioselective organic synthesis.^[1] More than 400 *cis*-cyclohexadienediols have been reported so far, with the methyl and halogen substituted ones (**1**, X = CH₃ or Cl, Br, I) being the most used for synthetic preparations.^[2]



Scheme 1. (A) Use of *cis*-cyclohexadienediols in enantioselective organic synthesis. (B) Regio- and stereoselectivity exhibited by wild type dioxygenases (1 and 2) and by the proposed mutants in this work.

Introduction

Enantiopure *cis*-cyclohexadienediols of type (**1**) have been extensively used as starting materials for organic synthesis of bioactive compounds and natural products (Scheme 1A). The useful array of functional groups present in (**1**) allows the use of regio- and stereocontrolled organic transformations resulting in short

These compounds are prepared from the corresponding arenes using Rieske non-heme iron dependent dioxygenases, which are responsible for the first step in the microbial degradation of aromatic arenes.^[3] To date, no other non-biocatalytic chemical method

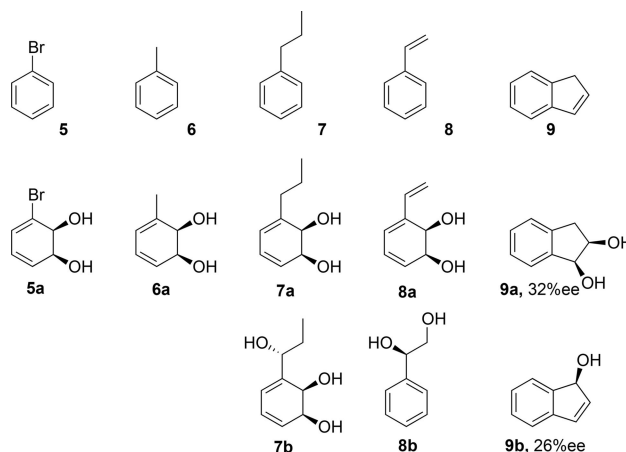
for their production at a preparative scale is known.^[4] Rieske non-heme iron dependent dioxygenases are multicomponent enzymes constituted by a reductase, an oxygenase and in some cases a ferredoxin, and are well known for their ability to activate molecular oxygen to oxidize organic compounds.^[3d] Besides the dioxygen addition to aromatic rings, Rieske dioxygenases are also able to catalyse other reactions, such as sulfoxidation, benzylic oxidation, dehydrogenation, and O- and N-dealkylations.^[5] The oxygen activation process occurs in the oxygenase component that contains a Rieske-type [2Fe–2S] cluster and a mononuclear non-heme iron in the active site.^[3c] Rieske dioxygenases are classified considering the homology between the alpha subunits of the oxygenase component, as well as the scope of arenes that are accepted for the dioxygenation process. Five classes are described: 1. Phthalate, 2. Benzoate, 3. Naphthalene, 4. Toluene and Bi-Phenyl and 5. Salicylate Dioxygenases.^[6]

Toluene Dioxygenase (TDO) is the enzymatic complex that has been used to produce the vast majority of the *cis*-cyclohexadienediols used for synthetic applications.^[1a,d] The biotransformation of arenes using this enzyme is carried out using whole cell biocatalysis with mutant organisms (*P.putida* F39/D, *P.putida* UV4) or recombinant strains overexpressing the TDO genes.^[1a] A recent publication by our group describes the biotechnological procedure to obtain 35 g/L of *cis*-3-bromocyclo-3,5-hexadiene-1,2-diol using the recombinant *E. coli* JM109 (pDTG601).^[7]

The TDO enzymatic system admits a high structural diversity of substrates, and the dioxygenation reaction is highly regio- and stereoselective.^[1a] Regarding monosubstituted benzene derivatives, dioxygenation always takes place at C2-C3 in a stereo-defined manner to afford diols of type (1) (except for fluorobenzene, where trace amounts of the regioisomeric diol at C3-C4 are also obtained) (Scheme 1B).^[8] This remarkable regio- and stereoselectivity for the aromatic dioxygenation is shared by most Rieske dioxygenases except for Benzoate dioxygenase (BzDO), which renders the dienediols of benzoic acids with the opposite stereochemistry and with the diol moiety in the position 1,2 (*ipso* addition) (see Scheme 1B, compound 2).^[1g]

The lack of regio- and stereodiversity of the dioxygenation process by TDO and related dioxygenases constitutes a clear drawback for the synthetic potential of the *cis*-cyclohexadienediols in organic synthesis, since the ready access to other regioisomers (e.g. dioxygenation product at C3-C4) or the enantiomer of (1) (see Scheme 1B, compounds 3 and 4), is precluded. Although synthetic protocols have been developed to obtain regio- and stereoisomers of (1),^[1a] a biocatalytic approach to produce them in a prepara-

tive scale is highly desirable. In addition, for certain substrates (as mono-substituted alkyl benzenes, indene and styrene) TDO presents poor chemoselectivity, since it can catalyze hydroxylations on the aromatic ring and in the side chain, rendering a mixture of compounds (see Scheme 2, compounds 7a–b, 8a–b and 9a–b)



Scheme 2. Substrates 5–9 and biotransformation products 5a–9b using wild type TDO. Unless stated, *ee* are >99% (data from literature for wild type TDO, see supporting information for specific references).

In this work, we propose to use site-directed mutagenesis in selected amino acids of the active site pocket of TDO to alter the chemo-, regio- and stereoselectivity of the dioxygenation of arenes. To the best of our knowledge, there are no previous studies about mutagenesis of TDO with the aim to alter the selectivity of the dioxygenation process. Previous reports about TDO mutants have used site-directed mutagenesis for determining the iron ligands in the active site, or directed evolution to improve the bioconversion of indene or to accept 4-picoline as a substrate.^[9]

Results and Discussion

Mutant's Selection and Design

To select the amino acid residues to be mutated in the active site of TDO, we used previous findings on the regio- and stereoselectivity of the dihydroxylation of arenes using Naphthalene (NDO) and Biphenyl Dioxygenases (BPDO), which share a high degree of homology with TDO.^[6] Although these enzymes have not been greatly used for synthetic purposes, they were deeply studied in the past for their potential application in bioremediation processes. In addition, NDO crystal structure has been early resolved,^[10]

which allowed for an in-depth study of its active site. Amino acid Phe352 of NDO was shown to be crucial for determining the regio- and stereoselectivity of the dihydroxylation of biphenyl, anthracene and phenanthrene.^[11] Although the overall enzymatic activity decreased in the studied mutants, changes in the Phe352 for medium size amino acids promoted biphenyl dioxygenation in the 3,4 position as the major product (with variable ee%).^[11c,12] Concerning BPDO, residues Ile335 and Thr376 were determined to alter the substrate scope and regioselectivity for the dihydroxylation of biphenyl.^[13] Previous studies using *Pseudomonas pseudoalcaligenes* KF707 BPDO, demonstrated that Ile335 was very important for determining substrate specificity and regioselectivity. The substrate scope for a range of polychlorinated biphenyls (PCB) was strongly associated with the amino acid side chain in this position. This was also in agreement with the reported biotransformation ability of the *Burkholderia cepacia* LB400 BPDO, which presents a phenylalanine instead of an isoleucine residue in this position.^[14] The I335F substitution markedly affected substrate specificity and regioselectivity, promoting dihydroxylation in the 3,4 position.^[13e,14b]

Regarding position 376 in BPDO, previous reports have shown that both residues threonine and asparagine are present at position 376 in different natural BPDO enzymes. All enzymes with broad substrate specificity contain asparagine at the 376 position, whereas the enzymes with narrow substrate specificity contain threonine at this site.^[15] Different mutations have been performed on this residue of BPDO. The introduction of amino acids smaller than Thr resulted in enzyme variants with reduced activity, while the inclusion of larger amino acids precluded substrate binding.^[13e]

An alignment performed among the abovementioned BPDOs (*B. xenovorans* and *P. pseudoalcaligenes* BPDO), NDO and TDO, allowed the identification of TDO residues equivalent to important positions on NDO and BPDO (Figure S0 Supplementary Information). Particularly, Phe366 corresponds to Phe352 in NDO, while Ile324 and Thr365 are equivalent to Ile335 and Thr376 from BPDO. Thus, these three residues were selected for site directed mutagenesis and I324F, T365N and F366V mutations were performed. Since the crystal structure of TDO was obtained in 2009,^[16] we could identify the selected residues in the active site pocket of this enzyme (Figure 1).

Expression vectors for mutant enzymes I324F, T365N and F366V were obtained by quick change mutagenesis, using pDTG601 as template. The obtained expression vectors were transformed into *E. coli* JM109 yielding the whole cell biocatalysts for characterization. The different recombinant strains were grown in batch fermentation as previously

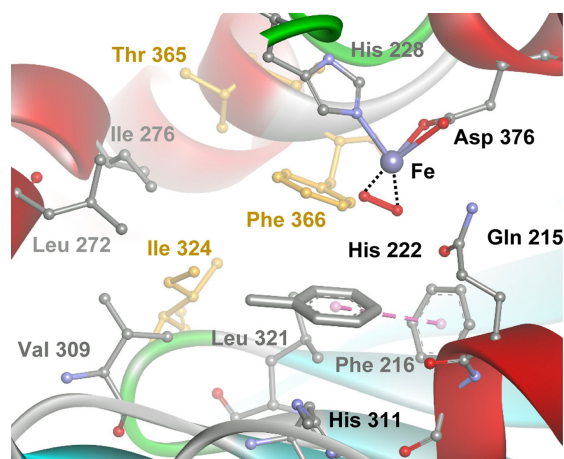


Figure 1. Active site of TDO loaded with O₂ and toluene. Selected amino acids I324, F366 and T376 for site-directed mutagenesis are shown in yellow. Color code: C (grey), N (blue), O (red), Fe (purple).

described,^[7] and cells were collected at stationary phase to perform resting cell assays (see experimental section).

Substrates

Five substrates were selected for characterization of the different mutant enzymes: toluene, bromobenzene, propylbenzene, styrene and indene (Scheme 2, 5–9). While all the selected substrates allowed us to detect changes in enzymatic activity and regio- and stereoselectivity of the different mutants, substrates (7–9) also permitted the evaluation of the chemoselectivity, since oxidation can occur at two different positions for these three substrates (for the wild type TDO, propylbenzene and indene renders the benzylic hydroxylation products in good yields (7b, 9b), and styrene gives the dihydroxylation product in the side chain olefin, (8b).

Biotransformation Results

Results for the biotransformation of the mentioned substrates using the TDO mutants are described in Table 1. Regarding mutants I324F and T365N, a similar outcome in the biotransformation of all substrates was found except for indene (9). A general reduction in enzyme activity for bromobenzene (5) and toluene (6) was observed for both mutants, with almost complete loss of activity for (6), and a slight decrease in yield for (5). Interestingly, changes in chemoselectivity were observed with both substrates (7) and (8). Hydroxylation of the benzylic position for propylbenzene (7) was not detected for both cases, indicating that a change in substrate accommodation in the active site probably precludes this position from

Table 1. Biotransformation results using TDO mutants and bromobenzene, toluene, propylbenzene, styrene and indene as substrates.

Substrate	Product	TDO (wild type)			I324F			T365N			F366 V		
		% ^a	ee% ^b	a:b ^c	% ^a	ee% ^b	a:b ^c	% ^a	ee% ^b	a:b ^c	% ^a	ee% ^b	a:b ^c
5	5a	57	99	–	49	99	–	55	99	–	2	60	–
6	6a	19	–	–	nd	–	–	3	–	–	nd	–	–
7	7a	31	>99	77:23	12	>99	100:0	18	>99	100:0	nd	–	–
	7b	10	90	–	nd	–	–	nd	–	–	nd	–	–
8	8a	8	>99	85:15	3	>99	37:63	3	>99	24:76	nd	–	–
	8b	1	>99	–	5	54	–	11	>99	–	2	17	0:100
9	9a	5	33	42:58	nd	–	–	2	23	11:89	9	–9 ^d	100:0
	9b	7	29	–	nd	–	–	15	53	–	nd	–	–

^[a] Overall biotransformation yield determined by ¹H-NMR of the crude biotransformation mixture using 1,3-dinitrobenzene as internal standard.

^[b] Enantiomeric excess was determined using chiral HPLC (see experimental section).

^[c] a:b ratio was determined by ¹H-NMR of the crude biotransformation mixtures.

^[d] The minus sign indicates an inverted relation of enantiomers. nd=not detected.

being oxidised. We have recently reported a computational model for TDO that nicely explained and predicted the outcome of the biotransformation for mono and 1,4-disubstituted arenes.^[17] This model allowed us to gain reliable insights into the benzylic hydroxylation of monosubstituted alkyl arenes, explaining the reasons behind propylbenzene being a better substrate for benzylic oxidation than similar compounds with longer or shorter substituents. Optimal fit of this substrate in TDO active site, with its side chain facing residues Leu272, Val309 and Ile324, compels the benzylic carbon atom to be closer to the coordinated O₂ molecule. In the case of the mutant I324F, our model shows that the change for phenylalanine generates a steric hindrance for accommodating the substrate in the same position, and the benzylic carbon atom moves 1.5 Å further away from the O₂ molecule (Figure 2). This nicely explains the observed result for I324F mutant, for which the benzylic oxidation was not detected.

Mutants I324F and T365N also presented an interesting behaviour with styrene (**8**). Although dihydroxylation of the aromatic ring was also reduced for this substrate for both mutants, dihydroxylation of the alkene on the side chain increased five folds for I324F, and ten times for T365N compared to the wild type enzyme. This implies a big change in chemoselectivity, favouring formation of the side chain diol while in the wild type the dioxygenation in the aromatic ring is preferred. Regarding the enantioselectivity for the dihydroxylation of the side chain, both mutants displayed different results. In the case of I324F enantioselectivity was changed from >99% to 54%, while for T365N it remained unchanged (>99%). This indicates that Ile 324 is an important residue for determining the stereoselectivity of dihydroxylation of some substrates.

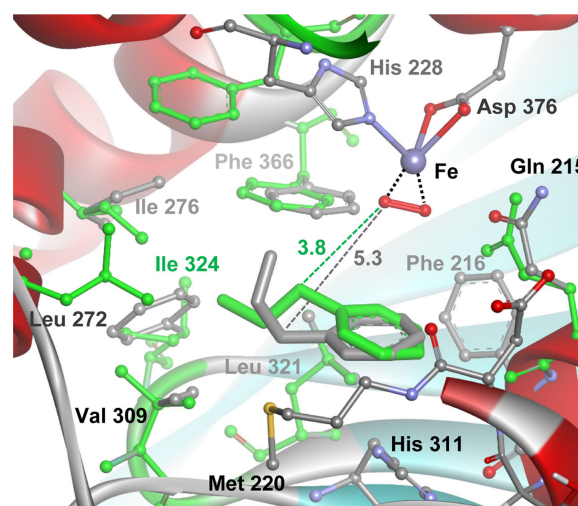


Figure 2. Propylbenzene docked into the active site of wild-type (green) or I324F (grey) TDO. As it can be seen, the benzylic position of propylbenzene is further away from the O₂ molecule for I324F (distances are shown in Å). Color code: C (grey), N (blue), O (red), Fe (purple), S (yellow).

A docking study of styrene with TDO and I324F mutant, based on our model,^[17] sheds light on the observed difference in chemoselectivity (Figure 3). In the wild type enzyme, 85% of the formed diols corresponds to dihydroxylation of the aromatic ring. The docking studies revealed that styrene accommodates in the active site at an ideal distance from the molecular O₂, favouring dihydroxylation of the aromatic ring in wild type TDO. The presence of a larger residue at position 324, displaces styrene ring from its coplanar geometry with molecular O₂, disfavoring its oxidation. Additionally, the styrene side chain comes closer to the reactive O₂ molecule which could

account for the observed increment in the yield of side chain dihydroxylation.

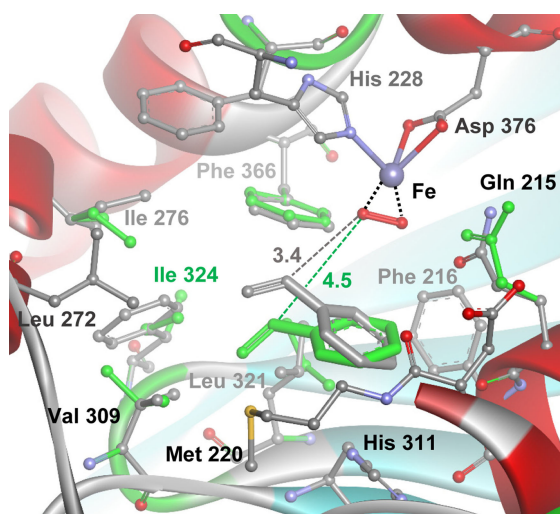


Figure 3. Styrene docked into the active site of wildtype (green) or I324F (grey) TDO. The benzylic carbon atom is nearer to the O₂ molecule for I324F (distances in Å). Color code: C (grey), N (blue), O (red), Fe (purple), S (yellow).

As mentioned before, the main difference between I324F and T365N was found in the biotransformation of indene (**9**). While I324F showed no activity for this substrate, T365N doubled the production of (**9b**), while reducing by half the production of (**9a**). In the case of I324F, our model shows some trends that could explain the lack of reaction of indene with this mutant. The introduction of a phenylalanine bulky residue at position 324 (Figure 1) destabilizes the binding position for indene favouring different orientations (see table S4 supporting info). This suggests that indene is probably loosely bound into the active site of I324F, which can explain the loss of enzymatic activity.

The outcome for the biotransformation of (**7**), (**8**) or (**9**) with the mutant T365N cannot be explained by the model. The mutation at position 365 does not produce a significant change nearby the substrate (see Figure 1), and since the protein backbone is fixed during the docking runs, our model does not consider any protein structural or electronic changes that may be involved. In order to rationalize this phenomenon, we are now carrying out molecular mechanics and DFT optimization calculations on mutant T365N. These results will be published in due course.

Overall, although we did not detect any change in regioselectivity for TDO I324F and T365N when tested with substrates (**5–9**), we found that these residues are indeed very important for determining chemoselectivity of the enzyme. Both amino acids also modulate the enantioselectivity for some substrates. The importance of these residues in enzyme activity

agrees with previous results obtained with BPDO.^[13c,e,14–15]

The TDO F366V mutant presented a drastic reduction in enzyme activity, larger than those observed for any other mutant. Indeed, the F366V variant was not capable of dihydroxylating the aromatic ring for substrates (**6**), (**7**) and (**8**), showing only 2% conversion for bromobenzene (**5**), the best substrate for the wild type biocatalyst. This general decrease in enzyme activity could be correlated, according to our model, with a general increment in the estimated binding ΔG , due to the decrease in substrate-receptor lipophilic interactions (see Table S4–S8). When the Phe366 residue is exchanged for valine, the structural changes in the active site upon mutation are significant (see for example Figure S7c), dramatically increasing its size. In general, this can be associated with more variation among the docking solutions (Tables S4–S8; an exception to this trend is toluene), which in turn may imply that substrates are loosely associated to the active site, and reaction become less likely to occur.

It is noteworthy that this mutation drastically affected the enantioselectivity of the enzyme, lowering the enantiomeric excess for the formation of (**5a**) from >99% to 60% (Table 1). Our model offers some answers concerning this change in the F366V enantioselectivity during bromobenzene dihydroxylation. According to the docking results shown in Figure S4b, different orientations of the substrate into the active site were found, which place the bromine atom almost in the opposite direction from the usual orientation, and can in principle give rise to the respective enantiomer. Remarkably enough, the calculated enantiomeric excess is 100% for the wildtype TDO and 65% for F366V mutant (Table S5), in excellent agreement with the experimental values (99 and 60%, respectively). The change in enantioselectivity for F366V was also observed for the preparation of (**8b**), (**9a**) and (**9b**). This mutant can then provide an interesting foundation to build up an enzyme with opposite stereoselectivity, using saturation mutagenesis in phenylalanine 366 or combining the F366V mutation with others that anchor the substrate in the opposite direction.

Intriguingly, while this mutant presented almost null activity for the hydroxylation of the aromatic ring, that was not the case for the oxidation of substrates (**8**) and (**9**) in non-aromatic positions. Production of (**8b**) and (**9a**) were doubled with this mutant, relative to the wild type TDO. These results indicate that the F366V TDO mutant did not lose the hydroxylation capability, but drastically changed its chemo and enantioselectivity.

When styrene is docked into the active site of F366V, new solutions are found that place the benzylic carbon near the O₂ molecule (Table S8 and Fig-

ure S7c). This phenomenon is much more pronounced than for the wild type TDO, and explains the better yield formation of (**8b**).

In the case of indene, the computational model indicates that the orientation compatible with the formation of (**9b**) for the wildtype enzyme, was not longer found for the F366V mutant (Table S4). This suggests that the indene monohydroxylation ability of TDO can be suppressed by the F366V mutation, in agreement with the experimental findings. Several efforts have been oriented to the development of TDO mutants that favoured formation of indene diol (**9a**) over the monooxygenation product (**9b**).^[18] Interest in this product relates to its use as a precursor in the synthesis of the antiviral agent Indinavir. Previous efforts have developed a TDO variant that accumulated five different mutations and reduced the formation of 1-indenol from 60% to 20% (showing a decreased overall catalytic activity). The F366V mutant reported here, renders exclusively the diol (**9a**) in an increased yield in contrast to the wild type enzyme (showing a better overall effect than the reported accumulation of five mutations mentioned before). In agreement with this previously reported TDO mutant, the F366V enzyme variant also affected the stereoselectivity of the reaction favouring the opposite enantiomer of (**9a**) compared to that produced using the wild type enzyme. These results show the importance of Phe366 on the search of an adequate biocatalyst for the synthesis of Indinavir and can be used as a foundation for further studies.

The effect of F366V mutation on the enantioselectivity is much larger than the one observed for the F352V substitution in NDO. Additionally, Phe352 position in NDO was shown to have an important effect on the regioselectivity of this enzyme. Both NDO mutants, F352V and F352L, favoured dihydroxylation in the 3,4 position for biphenyl and phenanthrene. The authors argued that stronger effects were associated to the bulkier substrates since they are likely to come in closer contact with all amino acids at the active site. This could also be the case for our mutants, where larger changes in chemoselectivity are associated to bulkier substrates (**8**) and (**9**); however, changes in regioselectivity were not observed with any of the tested substrates.

The possibility of having different substrate orientations in the active site could explain why a mixture of stereoisomers is observed during some of the biotransformations, rather than an enantiomerically pure product. It could also explain the switch on chemoselectivity. Even though our docking model gave us some answers, the computational assessment of this phenomenon for the most flexible substrates is not straightforward. It is highly possible that the side chain of substrates (**7**) and (**8**) can be rearranged before the dihydroxylation at the C=C double bond or

the monohydroxylation at the benzylic position takes place. This complex scenario can only be satisfactorily modelled by a higher-level computational model based on molecular mechanics or electronic structure methods. We are now starting to work on this issue, trying to rationalize the TDO mechanism of action.

Conclusion

Three different TDO mutants have been developed through site directed mutagenesis, and the effects of the different mutations have been analysed for the biotransformation of substrates (**5–9**) using our previously reported computational model. None of the developed mutants showed a variation in the regioselectivity of arene dihydroxylation. However, chemo- and enantioselectivity were largely affected in a substrate dependent manner.

Drastic changes in chemoselectivity were observed for the biotransformation of propylbenzene and styrene with I324F and T365N mutants, indicating that these positions are important for determining the orientation of the substrate in the active site and the overall outcome of the biotransformation. In the case of I324F mutation, the inserted phenylalanine residue is much bulkier than the isoleucine amino acid. In this regard, the substrates bearing large and flexible side chains (propylbenzene) can only accommodate them as in Figure 2, making the carbon atom at the benzylic position further away from the coordinated O₂ molecule, and preventing the monohydroxylation from taking place. When the chain is short and rigid (styrene), the Phe324 residue pushes and tilts the substrate towards the O₂ molecule, favouring the oxidation of the olefin against the dioxygen addition to the aromatic ring (Figure 3).

The most dramatic changes in enzyme activity were observed for the F366V variant. This mutation largely affected both the yield and the enantioselectivity of the enzyme, lowering the enantiomeric excess for the formation of (**5a**) from >98% to 60%. The calculated enantiomeric excesses are in excellent agreement with these values, which adds further evidence on the satisfactory performance of the developed computational model. This mutant can then provide an interesting foundation to build up an enzyme with opposite stereoselectivity, which will constitute a nice tool in organic synthesis. Furthermore, F366V presented a switch in chemoselectivity for the oxidation of indene, yielding (**9a**) as the only product. This is extremely interesting for the biocatalytic preparation of Indinavir.

Overall, our results shed light on the importance of Ile324, Thr365 and Phe366 residues in determining the chemo- and enantioselectivity of toluene dioxygenase. The reported results constitute an interesting basis for further studies in the field.

Experimental Section

Strains and Growth Conditions

E. coli JM109 was acquired from New England BioLabs (Ipswich, MA, USA), and *E. coli* JM109 (pDTG601) was generously donated by Prof. David T. Gibson (1938–2014). All his strain collections are currently managed by Prof. Rebecca Parales (University of California, Davis). *E. coli* JM109, *E. coli* JM109 (pDTG601) and the three mutants *E. coli* JM109 (pTDO^M) were properly stored in cryovials at -70°C .

E. coli JM109 was routinely cultivated in Luria–Bertani (LB) broth or on LB agar plates at 37°C . Recombinant strains *E. coli* JM109 (pDTG601) and the three mutants *E. coli* JM109 (pTDO^M) were grown in LB agar plates or LB broth supplemented with ampicillin $200\ \mu\text{g}/\text{mL}$. Mineral Salts Broth (MSB) was used as the culture media for growing *E. coli* JM109 (pDTG601) and the three mutants *E. coli* JM109 (pTDO^M) in batch fermentations.

Chemicals and Molecular Biology Reagents

Biotransformation substrates **5** to **9** were purchased from Sigma Aldrich (St Louis, MO, USA) and were used without further purification. Molecular biology reagents were purchased from New England Biolabs (Ipswich, MA, USA) and Thermo Fisher Scientific (Waltham, MA, USA). Solvents for product purification were distilled prior to use. HPLC n-hexane was acquired from Pharmco-Aaper and HPLC 2-propanol was acquired from Carlo Erba Reagents.

DNA Manipulation

Standard procedures were used for DNA manipulation.^[19] Plasmid DNA was purified using commercial chromatography kits (Thermo Fisher Scientific). Phusion[®] High-fidelity DNA polymerase (New England Biolabs) was used according to the manufacturers' instructions. PCR amplifications were performed in a GeneAMP PCR system 2400 (Perkin Elmer) using adequate cycling periods and DNA samples were routinely analyzed by agarose gel electrophoresis (Sambrook 2001). Transformations of electrocompetent cells were performed on a BioRad MicroPulser[™] Electroporator.

Generation of TDO Variants (TDO^M): I324F, T365N, F366V

Mutant variants of TDO were constructed using a modification of Quikchange[®] method (Agilent Technologies). Amplifications with Phusion High Fidelity DNA polymerase (New England Biolabs) were performed on a GeneAMP PCR system 2400 (Perkin Elmer) using plasmid pDTG601 as a template and the primers listed in Table S1 (see supporting info).

After amplification, samples were digested with *DpnI* (Fermentas) for 3 h at 37°C . DNA was precipitated with ethanol and stored at -20°C for at least 1 hour. DNA was recovered in water and used to transform *E. coli* JM109 electrocompetent cells prepared in our lab according to New

England Biolabs protocol. Mutations were confirmed by sequencing in Macrogen, Korea.

Whole-Cell Biotransformation

All mutants and the wild type strain were grown in a 5 L bioreactor (Sartorius Biostat A plus) using a modification of our previously published procedure.^[7] Fresh plates of *E. coli* JM109 (pDTG601) and *E. coli* JM109 (pTDO^M) were streaked from frozen stocks, and a single colony was used to inoculate 5 mL of LB-Amp which was incubated in orbital shaker overnight (150 rpm, 37°C). Two 500 mL Erlenmeyer flasks containing 150 mL of MSB medium were inoculated with 1.5 mL of the grown culture, and grown for 12 h in orbital shaker at 37°C , 150 rpm. Both entire cultures were used to inoculate 2.5 L of defined mineral salt media in a bioreactor (Sartorius Biostat A plus), and the system was set to 500 rpm, 30°C , and air flow rate of 4 L/min, and a pulse of antifoam agents (Aldrich's Antifoam Y: Silicone dispersion in water 1:1) was added at the beginning of the run. The pH value was controlled automatically to 6.8 by addition of ammonium hydroxide during the whole process. A glucose fed-batch started 6 hours after inoculation by adding glucose (0.7 g/mL solution) from an initial rate of 0.08 mL/min to 0.54 mL/min in a 20 h period. IPTG was added to a final concentration of 10 mg/L 12 hours after inoculation to induce enzyme expression, and stirrer speed was set to 900 rpm. After the culture reached the stationary phase (c.a. 26 h, 30 g/L cdw aprox) cells were harvested by centrifugation (4000 rpm, 20 min, 4°C), and the pellet was resuspended in isotonic phosphate buffer (KH_2PO_4 3 g/L, NaHPO_4 12 g/L, NaCl 0.7 g/L) to a final $\text{OD}_{600}=30$. Biotransformations were performed using resting cells, thus, 100 mL of this cell suspension were placed in 500 mL Erlenmeyer flasks and supplemented with glucose to a final concentration of 5 g/L. Neat substrates were added to a final concentration of 10 mM and incubated overnight at 28°C , 150 rpm. Resting cell cultures were centrifuged at 4000 rpm, 4°C , 20 min, the supernatant was collected and the cells were properly disposed. The supernatant was lyophilized, and the solid was washed with $3 \times 100\ \text{mL}$ ethyl acetate. The organic solvent was evaporated *in vacuo* to afford a reaction crude that was analysed by $^1\text{H-NMR}$ for yield determination (vide infra). Products were properly purified by preparative thin layer chromatography (silica gel 60F-254 plates and visualized by UV light 254 nm) or flash column chromatography using silica gel (Kieselgel 60, EM reagent, 230–400 mesh). Pure products were identified by $^1\text{H-NMR}$ and compared with literature data (vide infra)

Proton chemical shifts (δ) for the products obtained for the wild type biotransformation are described below:

5a.

Cis-(1*S*,2*S*)-3-bromocyclohexa-3,5-diene-1,2-diol^[20]

$^1\text{H-NMR}$ (400 MHz, CDCl_3): δ 6.37 (d, $J=6\ \text{Hz}$, 1H), 5.88 (dd, $J=9, 3\ \text{Hz}$, 1H), 5.79 (ddd, $J=9, 6, 3\ \text{Hz}$, 1H), 4.47 (dt, 7, 3, 3 Hz 1H), 4.34 (d, $J=7\ \text{Hz}$, 1H).

7a.

Cis-(1S,2R)-3-propylcyclohexa-3,5-diene-1,2-diol^[21]

¹H-NMR (400 MHz, CD₃COCD₃): δ 5.85 (ddd, *J*=10, 5, 2 Hz, 1H), 5.71–5.66 (m, 2H), 4.22 (s, 1H), 3.95 (t, *J*=5 Hz, 1H), 3.81 (s, 1H), 3.59 (s, 1H), 2.30–2.23 (m, 1H), 2.17–2.06 (m, 1H), 1.63–1.43 (m, 2H), 0.93 (t, *J*=7 Hz, 3H).

7b. Cis-(1S,2R)3-[(R)1'-hydroxyethyl]cyclohexa-3,5-diene-1,2-diol^[21]

¹H-NMR (400 MHz, CD₃COCD₃): δ 5.90–5.87 (m, 2H), 5.73–5.70 (m, 1H), 4.22 (m, 1H), 4.17 (m, 1H), 3.80 (brs, 1H), 3.50 (brs, 1H), 1.75 (m, 1H), 1.58 (m, 1H), 0.93 (m, 3H).

8a. Cis-2,3-dihydroxy-1-vinylcyclohexa-4,6-diene^[22]

¹H-NMR (400 MHz, CD₃COCD₃): δ 6.42 (dd, *J*=16, 8 Hz, 1H), 5.97–5.91 (m, 2H), 5.80 (d, *J*=9, 1H), 5.50 (d, *J*=18 Hz, 1H), 5.12 (d, *J*=11 Hz, 1H), 4.41–4.37 (m, 1H), 4.32–4.28 (m, 1H), 3.98 (d, *J*=8 Hz, 1H), 3.63–3.61 (m, 1H).

8b. (R)1-Phenyl-1,2-ethanediol^[23]

¹H-NMR (400 MHz, CD₃COCD₃): δ 7.43–7.37 (m, 2H), 7.35–7.29 (m, 2H), 7.28–7.21 (m, 1H), 4.72 (dd, *J*=8, 4 Hz, 1H), 4.34 (d, *J*=4 Hz, 1H), 3.85 (dd, *J*=7, 5 Hz, 1H), 3.66–3.62 (m, 1H), 3.57–3.51 (m, 1H).

9a. Cis-(1S,2R)-indandiol^[24]

¹H-NMR (400 MHz, CDCl₃): δ 7.51–4.43 (m, 1H), 7.32–7.25 (m, 3H), 5.00 (s, 1H), 4.50 (s, 1H), 3.14 (dd, *J*=16, 6 Hz, 1H), 2.98 (dd, *J*=16, 4 Hz, 1H), 2.80 (brs, 1H), 2.69 (brs, 1H).

9b. (1S)-Indenol^[24]

¹H-NMR (400 MHz, CDCl₃): δ 7.54 (d, *J*=7, 1H), 7.46–7.44 (m, 4H), 6.76 (d, *J*=6 Hz, 1H), 6.43 (dd, *J*=6, 2 Hz, 1H), 5.21 (s, 1H).

Analytical Methods

Biotransformation Yields

The biotransformation crudes obtained as described previously were analysed by ¹H-NMR (Bruker Avance DPX-400) using *m*-dinitrobenzene as an internal standard for yield determination.

Enantiomeric Excess Determination

Chiral normal phase HPLC was performed on a Shimadzu Prominence Liquid Chromatograph LC-20AT using chiral columns according previous reports.^[25] Lux[®] Cellulose-1, (250 mm length, 4.6 mm diameter, 5 μm particle size – Phenomenex[®]) column was used to separate the enantiomers of 1-phenyl-1,2-ethanediol (**8b**) and 1-indenol (**9b**), and Chiralcel[®] OJ–H column (250 mm length, 4.6 mm diameter, 5 μm particle size – Daicel Chemical Industries, Ltd.) was

used to separate the enantiomers of **5a**, **7a**, **7b**, **8a** and **9a** (see supporting information for the detailed retention times for each enantiomer). Analytical conditions for separation of 1-phenyl-1,2-ethanediol and 1,2-indandiol were optimized by analysis of the chemically synthesized racemic mixture.^[26] The typical injection volume was 20 μl and chromatograms were monitored at maximum absorption wavelength for each product (see supporting info). Assignment of the absolute configuration was based on comparison with previously reported results for wild type TDO.

Docking Calculations

Molecular-docking experiments were carried out according to Vila *et al.*^[17] by using the GOLD docking program (v 4.1.2).^[27] Various rotamers were considered for some of the amino acids in the binding site: Glu 215 (8), Phe 216 (3), Asp 219 (4), Met 220 (4), Ile 276 (4), Val 309 (3), His 311 (4), Leu 321 (3), Ile 324 (3), Phe 366 (2). The mutated residues and those in contact with them and with the substrate at the same time were set free to move during the docking runs. Each substrate was docked 40 times, and the docking modes that achieved the highest Goldscore fitness were retained and compared. The most stable docking poses were selected considering the values of the ChemScore and Goldscore scoring functions.^[20,28] Other miscellaneous parameters were assigned the default values given by the GOLD program. The amino acid mutations and the rendering of the results were done with Discovery Studio Visualizer software.^[29]

Acknowledgements

Authors would like to thank the Agencia Nacional de Investigación e Innovación (ANII, Project Fondo Clemente Estable 103485), CSIC Grupos I+D 981 (UdelaR) and PEDECIBA Química for financial support. M. A. Vila thanks UdelaR-Comisión Académica de Posgrado for a Ph.D. scholarship. The authors would like to thank Daniel Galdrán (visiting student from Universitat de Valencia-Spain) for the preparation of the racemic diols (8b) and (9a).

References

- [1] a) D. Gonzalez, D. T. Gibson, T. Hudlicky, *Aldrichimica acta* **1999**, 32, 35; b) M. G. Banwell, A. J. Edwards, G. J. Harfoot, K. A. Jolliffe, M. D. McLeod, K. J. McRae, S. G. Stewart, M. Vogtle, *Pure Appl. Chem.* **2003**, 75, 223; c) R. A. Johnson, *Microbial arene oxidations*, Vol. 63, John Wiley and Sons, Inc., **2004**; d) T. Hudlicky, J. W. Reed, *Synlett* **2009**, 0685; e) M. G. Banwell, A. L. Lehmann, S. M. Rajeev, A. C. Willis, *Pure Appl. Chem.* **2011**, 83, 411; f) M. G. Banwell, N. Gao, X. Ma, L. Petit, L. V. White, *Pure Appl. Chem.* **2012**, 84, 1329; g) S. E. Lewis, *Chem. Commun.* **2014**, 50, 2821; h) S. Lewis, in *Asymmetric Dearomatization Reactions* (Ed.: S.-L. You), Wiley-VCH Verlag GmbH & Co. KGaA, New York, **2016**, pp. 279–346.

- [2] D. Gamenara, G. A. Seoane, P. Sáenz-Mendez, P. Domínguez de María, John Wiley & Sons, Inc., **2013**, pp. 251.
- [3] a) P. C. A. Bruijninx, G. van Koten., J. M. Klein Gebbink, *Chem. Soc. Rev.* **2008**, *37*, 2716; b) T. D. H. Bugg, S. Ramaswamy, *Curr. Opin. Chem. Biol.* **2008**, *12*, 134; c) D. Gamenara, G. A. Seoane, P. Saenz-Méndez, P. Dominguez de Maria, *Redox Biocatalysis: Fundamentals and Applications*, John Wiley & Sons, **2013**; d) S. M. Barry, G. L. Challis, *ACS Catal.* **2013**, *3*, 2362.
- [4] Y. Feng, C. Y. Ke, G. Xue, L. Que, *Chem. Commun.* **2009**, 50.
- [5] a) S. M. Resnick, K. Lee, D. T. Gibson, *J. Ind. Microbiol.* **1996**, *17*, 438; b) D. R. Boyd, N. D. Sharma, B. E. Byrne, M. V. Hand, J. F. Malone, G. N. Sheldrake, J. Blacker, H. Dalton, *J. Chem. Soc., Perkin Trans. 1* **1998**, 1935; c) D. R. Boyd, N. D. Sharma, N. I. Bowers, J. Duffy, J. S. Harrison, H. Dalton, *J. Chem. Soc., Perkin Trans. 1* **2000**, *1*, 1345; d) D. R. Boyd, N. D. Sharma, B. E. Byrne, S. A. Haughey, M. A. Kennedy, C. C. R. Allen, *Org. Biomol. Chem.* **2004**, *2*, 2530.
- [6] R. E. Parales, S. M. Resnick, in *Pseudomonas, Volume 4*, Springer, The Netherlands, **2006**.
- [7] M. A. Vila, M. Brovotto, D. Gamenara, P. Bracco, G. Zinola, G. Seoane, S. Rodríguez, I. Carrera, *J. Mol. Catal. B: Enzym.* **2013**, *96*, 14.
- [8] a) D. R. Boyd, N. D. Sharma, G. P. Coen, F. Hempentstall, V. Ljubez, J. F. Malone, C. C. R. Allen, J. T. G. Hamilton, *Org. Biomol. Chem.* **2008**, *6*, 3957; b) D. R. Boyd, N. D. Sharma, M. V. Hand, M. R. Groocock, N. A. Kerley, H. Dalton, J. Chima, G. N. Sheldrake, *J. Chem. Soc., Chem. Commun.* **1993**, 974.
- [9] a) H. Jiang, R. E. Parales, N. A. Lynch, D. T. Gibson, *J. Bacteriol.* **1996**, 3133; b) N. Zhang, B. G. Stewart, J. C. Moore, R. R. Greasham, D. K. Robinson, B. C. Buckland, C. Lee, *Metab. Eng.* **2000**, *2*, 339; c) T. Sakamoto, J. M. Joern, A. Arisawa, F. H. Arnold, *App. Environ. Microbiol.* **2001**, *67*, 3882.
- [10] a) B. Kauppi, K. Lee, E. Carredano, R. E. Parales, D. T. Gibson, H. Eklund, S. Ramaswamy, *Structure* **1998**, *6*, 571; b) A. Karlsson, J. V. Parales, R. E. Parales, D. T. Gibson, H. Eklund, S. Ramaswamy, *Science* **2003**, *299*, 1039.
- [11] a) R. E. Parales, *J. Ind. Microbiol. Biotechnol.* **2003**, *30*, 271; b) R. E. Parales, K. Lee, S. M. Resnick, H. Jiang, D. J. Lessner, D. T. Gibson, *J. Bacteriol.* **2000**, *180*, 1641; c) R. E. Parales, S. M. Resnick, C.-L. Yu, D. R. Boyd, N. D. Sharma, D. T. Gibson, *J. Bacteriol.* **2000**, *182*, 5495.
- [12] R. E. Parales, K. Lee, S. M. Resnick, H. Jiang, D. J. Lessner, D. T. Gibson, *J. Bacteriol.* **2000**, *180*, 1641.
- [13] a) H. Suenaga, T. Watanabe, M. Sato, Ngadiman, K. Furukawa, *J. Bacteriol.* **2002**, *184*, 3682; b) J. Vézina, D. Barriault, M. Sylvestre, *J. Bacteriol.* **2007**, *189*, 779; c) M. Mohammadi, J.-F. Viger, P. Kumar, D. Barriault, J. T. Bolin, M. Sylvestre, *J. Biol. Chem.* **2011**, *286*, 27612; d) P. Kumar, M. Mohammadi, S. Dhindwal, T. T. My Pham, J. T. Bolin, M. Sylvestre, *Biochem. Biophys. Res. Commun.* **2012**, *421*, 757; e) H. Suenaga, M. Goto, K. Furukawa, *Appl. Microbiol. Biotechnol.* **2006**, *71*, 168.
- [14] a) F. Bruhlmann, W. Chen, *Biotechnol. Bioeng.* **1999**, *63*, 544; b) P. Kumar, M. Mohammadi, J. F. Viger, D. Barriault, L. Gomez-Gil, L. D. Eltis, J. T. Bolin, M. Sylvestre, *J. Mol. Biol.* **2011**, *405*, 531.
- [15] H. Suenaga, T. Watanabe, M. Sato, Ngadiman, K. Furukawa, *J. Bacteriol.* **2002**, *184*, 3682.
- [16] R. Friemann, K. Lee, E. N. Brown, D. T. Gibson, H. Eklund, S. Ramaswamy, *Acta crystallographica. Section D, Biological crystallography* **2009**, *65*, 24.
- [17] M. A. Vila, D. Umpiérrez, G. Seoane, S. Rodríguez, I. Carrera, N. Veiga, *J. Mol. Catal. B: Enzym* **2017**, <https://doi.org/10.1016/j.molcatb.2017.03.003>.
- [18] N. Zhang, B. G. Stewart, J. C. Moore, R. R. Greasham, D. K. Robinson, B. C. Buckland, C. Lee, *Metabolic Engineering* **2000**, *2*, 339.
- [19] J. Sambrook, D. W. Russell, *Molecular Cloning. A Laboratory Manual.*, 3rd ed., Cold Spring Harbor, New York, **2001**.
- [20] C. A. Baxter, C. W. Murray, D. E. Clark, D. R. Westhead, M. D. Eldrige, *Proteins: Structure, Function and Genetics* **1998**, *33*, 367.
- [21] D. R. Boyd, N. D. Sharma, N. I. Bowers, J. Duffy, J. S. Harrison, H. Dalton, *J. Chem. Soc., Perkin Trans. 1* **2000**, *1*, 1345.
- [22] T. Hudlicky, H. Luna, G. Barbieri, L. D. Kwart, *J. Am. Chem. Soc.* **1988**, *110*, 4735.
- [23] T. Hudlicky, E. E. Boros, C. H. Bores, *Tetrahedron: Asymmetry* **1993**, *4*, 1365.
- [24] L. P. Wackett, L. D. Kwart, D. T. Gibson, *Biochemistry* **1988**, *27*, 1360.
- [25] a) D. R. Boyd, N. D. Sharma, S. A. Barr, H. Dalton, J. Chima, G. Whited, R. Seemayer, *J. Am. Chem. Soc.* **1994**, *116*, 1147; b) D. R. Boyd, N. D. Sharma, G. P. Coen, P. J. Gray, J. F. Malone, J. Gawronski, *Chem. Eur. J.* **2007**, *13*, 5804; c) D. R. Boyd, N. D. Sharma, M. V. Hand, M. R. Groocock, N. A. Kerley, H. Dalton, J. Chima, G. N. Sheldrake, *J. Chem. Soc., Chem. Commun.* **1993**, 974.
- [26] C. Gally, B. M. Nestl, B. Hauer, *Angew. Chem. Int. Ed.* **2015**, *54*, 12952.
- [27] G. Jones, P. Willett, R. C. Glen, A. R. Leach, R. Taylor, *J. Mol. Biol.* **1997**, *267*, 727.
- [28] M. D. Eldrige, C. W. Murray, T. R. Auton, G. V. Paolini, R. P. Mee, *J. Comput. Aided Mol. Des.* **1997**, *11*, 425.
- [29] 2.5.5.9350 ed., Accelrys Software Inc., **2009**.